Intracellular targeting and homotetramer formation of a truncated inositol 1,4,5-trisphosphate receptor–green fluorescent protein chimera in *Xenopus laevis* oocytes: evidence for the involvement of the transmembrane spanning domain in endoplasmic reticulum targeting and homotetramer complex formation

Lee G. SAYERS*†‖¶, Atsushi MIYAWAKI*, Akira MUTO*‡, Hiroshi TAKESHITA*, Akitsugu YAMAMOTO§, Takayuki MICHIKAWA*, Teiichi FURUICHI* and Katsuhiko MIKOSHIBA*†‡

*Department of Molecular Neurobiology, Institute of Medical Science, University of Tokyo, 4-6-1 Shiroganedai, Minato-ku, Tokyo 108, †Molecular Neurobiology Laboratory, the Institute of Physical and Chemical Research (RIKEN), 3-1-1, Koyadai, Tsukuba Life Science Centre, Ibaraki 305, ‡Calciosignal Net Project, Exploratory Research for Advanced Technology (ERATO), JRDC 2-9-3 Shimo-Meguro, Tokyo 153, and §Department of Physiology, Kansai Medical University, 1- Fumizonocho, Moriguchi-shi, Osaka 570, Japan

In an attempt to define structural regions of the type I inositol 1,4,5-trisphosphate [Ins(1,4,5)P_3] receptor [Ins(1,4,5)P_3R] involved in its intracellular targeting to the endoplasmic reticulum (ER), we have employed the use of green fluorescent protein (GFP) to monitor the localization of a truncated Ins(1,4,5)P_3R mutant containing just the putative transmembrane spanning domain and the C-terminal cytoplasmic domain [amino acids 2216–2749; termed inositol trisphosphate receptor(ES)]. We expressed a chimeric GFP–Ins(1,4,5)P_3R(ES) fusion protein in *Xenopus laevis* oocytes, and used fluorescence confocal microscopy to monitor its intracellular localization. Fluorescence confocal microscopy data showed an intense fluorescence in the perinuclear region and in a reticular-network under the animal pole of the oocyte, consistent with the targeting of expressed GFP–Ins(1,4,5)P_3R(ES) to perinuclear ER and ER under the animal pole. These findings are consistent with the intracellular localization of the endogenous *Xenopus* Ins(1,4,5)P_3R shown previously. Furthermore, electron microscopy data indicate that expressed GFP–Ins(1,4,5)P_3R(ES) is in fact targeted to the ER. Sodium carbonate extraction of microsomal membranes and cross-linking experiments indicate that the expressed chimeric protein is in fact membrane anchored and able to form a homotetrameric complex. Our data provides evidence that Ins(1,4,5)P_3R(ES) constitutes the membrane spanning domain of the Ins(1,4,5)P_3R and is able to mediate homotetramer formation, without the need for the large N-terminal cytoplasmic domain. Furthermore, the localization of GFP–Ins(1,4,5)P_3R(ES) on the ER indicates that an ER retention/targeting signal is contained within the transmembrane spanning domain of the inositol trisphosphate receptor.

INTRODUCTION

Inositol 1,4,5-trisphosphate [Ins(1,4,5)P_3] represents a ubiquitous second messenger responsible for the release of Ca^{2+} from intracellular stores [1]. Ins(1,4,5)P_3, following its release into the cytosol, binds to an intracellular Ca^{2+} channel, the Ins(1,4,5)P_3 receptor [Ins(1,4,5)P_3R], which in turn mediates the release of Ca^{2+} into the cytosol [2]. The Ins(1,4,5)P_3R thus functions to transduce the binding of extracellular ligands at the cell surface into an intracellular Ca^{2+} signal. The structure of the Ins(1,4,5)P_3R can be divided into three functionally distinct domains: (1) an N-terminal cytoplasmic Ins(1,4,5)P_3 binding domain, (2) a regulatory domain linking the N-terminal Ins(1,4,5)P_3 binding site to the (3) C-terminal channel domain [3]. Molecular cloning studies have revealed that there are at least three isoforms of the Ins(1,4,5)P_3R derived from distinct genes: types I, II and III [4], which exhibit different tissue distributions [5] and are anticipated to have different regulatory properties. Type I Ins(1,4,5)P_3R is predominantly found in the central nervous system, being particularly enriched in the Purkinje cells of the cerebellum [6–9], and types II and III are predominantly found in peripheral tissues [10].

Cross-linking studies [11], electron microscopic observations [12] and sucrose density gradient centrifugation experiments [13] have demonstrated the ability of the Ins(1,4,5)P_3R to form a homotetrameric complex, and recently it has been shown that distinct isoforms of the Ins(1,4,5)P_3R are able to combine and form a single heterotetrameric complex [14], further increasing the diversity of Ins(1,4,5)P_3-sensitive Ca^{2+} channels. Little information is available on the molecular mechanisms by which Ins(1,4,5)P_3Rs are able to form tetrameric complexes; however, it has previously been shown that removal of the transmembrane spanning domain leads to a loss of homotetramer formation, and a mutant containing just the N-terminal cytoplasmic domain and cytoplasmic C-terminal domain was able to form a dimeric complex [15]. The identification of intracellular Ca^{2+} stores which are sensitive and insensitive to Ins(1,4,5)P_3 has revealed that the organization of intracellular Ca^{2+} stores is complex [16].

Abbreviations used: Ins(1,4,5)P_3R, inositol 1,4,5-trisphosphate receptor; GFP, green fluorescent protein; ER, endoplasmic reticulum; MBS, modified Barth's solution; DTT, dithiothreitol; mAb, monoclonal antibody; DST, disuccinimidyl tartrate; wt, wild-type.

‖ Present address: Protein Phosphorylation Laboratory, Imperial Cancer Research Fund, P.O. Box 123, Lincolns Inn Fields, London WC2A 3PX, U.K.
¶ To whom correspondence should be addressed.

Indeed, in the past much controversy has surrounded the identity of Ins(1,4,5)P_3-sensitive Ca^{2+} stores. However, it is now generally accepted that the Ins(1,4,5)P_3R resides on specialized regions of the endoplasmic reticulum (ER), which in fact constitute Ins(1,4,5)P_3-sensitive Ca^{2+} stores [17]. To date, little is known about the mechanisms underlying the intracellular targeting of the Ins(1,4,5)P_3R to the ER, and indeed the targeting of ER-resident membrane proteins in general.

Here, in an attempt to define regions of the type I Ins(1,4,5)P_3R that are involved in intracellular targeting to the ER, we have employed the use of green fluorescent protein (GFP), originally isolated from the jellyfish *Aequorea victoria* [18], to monitor the intracellular localization of the mouse type I Ins(1,4,5)P_3R. Using PCR, we have created a chimeric GFP–Ins(1,4,5)P_3R fusion protein, which we expressed in *Xenopus laevis* oocytes. This chimeric construct contains only the putative transmembrane spanning region of the mouse type I Ins(1,4,5)P_3R [amino acids 2216–2749; named Ins(1,4,5)P_3R(ES)], with GFP linked to the N-terminus. Using both confocal and electron microscopy, we report that, like the endogenous *Xenopus* Ins(1,4,5)P_3R, this chimeric construct is targeted preferentially to the ER under the animal pole of the oocyte. Furthermore, we present data to show that this construct is membrane anchored and also able to form a homotetramer, providing evidence that the putative transmembrane spanning region of Ins(1,4,5)P_3R alone can mediate ER targeting and homotetrameric complex formation, without the requirement for the N-terminal cytoplasmic domain.

EXPERIMENTAL PROCEDURES

Plasmid construction

To construct the plasmid pMT3 GFP–Ins(1,4,5)P_3R(ES), the ES fragment (corresponding to amino acids 2216–2749) of mouse type I Ins(1,4,5)P_3R was excised from the full-length cDNA by *Eco*RI digestion, and subcloned into the *Eco*RI site of pBluescript SK(+). The coding region of S65T (GFP) was amplified by PCR, using 100 ng of the template pRSETB–S65T (Clonetech), 200 μM of each dNTP and 1 unit of *Pfu* DNA polymerase (Stratagene) in a final volume of 100 μl (30 cycles; denaturing temperature 95 °C for 3 min, annealing temperature of 55 °C for 2 min and extension temperature of 72 °C for 1 min). Two oligonucleotide primers used in the PCR reaction at a concentration of 1 μM were designed to contain an *Xba*I restriction enzyme site upstream (5′ end) of the S65T start codon, and a *Bam*HI site downstream of the coding region of S65T. This allowed the PCR fragment to be subcloned into the *Xba*I/*Bam*HI site in the multicloning region of pBluescript SK(+) Ins(1,4,5)P_3R(ES).

The PCR primers used were of the following sequence:
Upstream:
5′GAG TCT AGA GCC ACC ATG AGT AAA GGA GAA GAA CTT TTC3′
Downstream:
5′GTC GGA TCC TTT GTA TAG TTC ATC CAT GCC ATG3′
The 3′ downstream primer was designed to exclude the stop codon normally found at the 3′ end of the coding region of S65T. This enabled the translation of the entire S65T Ins(1,4,5)P_3R(ES) coding sequence. Following PCR, generated fragments were analysed by agarose gel electrophoresis and fragments of appropriate size were purified (Qiagen Spin PCR Purification kit) and digested with *Xba*I and *Bam*HI restriction enzymes. The fragment was then subcloned into pBluescript Ins(1,4,5)P_3R(ES).

Following subcloning of S65T into the *Xba*I and *Bam*HI sites of pBluescript SK(+) Ins(1,4,5)P_3R(ES), the entire S65T Ins(1,4,5)P_3R(ES) sequence was excised from pBluescript by digestion with *Not*I and *Kpn*I restriction enzymes, and subcloned into the *Not*I/*Kpn*I restriction enzyme sites of the mammalian expression vector pMT3 (Genetic Co.).

All PCR product sequences were confirmed by dideoxy DNA sequencing using Pharmacia's ALF Autoread DNA sequencing apparatus according to the manufacturers' instructions.

The introduction of the S65T PCR fragment into the *Xba*I/*Bam*HI restriction enzyme sites of pBluescript, upstream of Ins(1,4,5)P_3R(ES), generated six additional amino acids (Gly-Ser-Pro-Gly-Leu-Gln), which linked S65T to Ins(1,4,5)P_3R(ES). However, the PCR primers used were designed to minimize the generation of any extra amino acids and ensure the DNA sequence of Ins(1,4,5)P_3R(ES) was read in frame.

Procurement and microinjection of *X. laevis* oocytes

Ovarian fragments were surgically removed from adult female *X. laevis* (purchased from Hamamatsu Seibutsu Company, Shizuoka, Japan), anaesthetized by hypothermia, and were torn into small clumps and washed in modified Barth's solution (MBS) [19] (88 mM NaCl/1 mM KCl/2.4 mM $NaHCO_3$/10 mM Hepes (pH 7.5)/0.82 mM $MgSO_4$/0.33 mM $Ca(NO_3)_2$/0.41 mM $CaCl_2$). Fully grown stage VI oocytes (1.2–1.3 mm diameter) were obtained by manual defolliculation using watchmakers forceps, and maintained in MBS at 18 °C until microinjection.

Microinjection of individual oocytes was performed under light microscope using a nitrogen air pressure microinjector IM-200 (Narishige). Plasmid DNA, pMT3 GFP(S65T)–Ins(1,4,5)P_3R(ES) (approx. 1 ng), was microinjected into the nucleus of the oocyte by impaling the animal hemisphere with a microinjection needle (borosilicate glass rod of diameter 6 μm). All oocytes were maintained in MBS at 18 °C during and after all microinjection procedures.

Fluorescent measurements

After microinjection (2–3 days), individual oocytes were monitored for GFP fluorescence using a Zeiss laser scanning confocal microscope (objective lens ×10, Nikon) using the Carl Zeiss LSM software package provided. The focus of light was adjusted to the surface of the oocyte and the confocal aperture was fully opened to maximize the collection of light. Light of excitation wavelength 490 nm and emission 510 nm was used to visualize GFP fluorescence from microinjected oocytes. Oocytes positive in GFP fluorescence were selected for further experiments. Oocytes microinjected with vector pMT3 alone (vector control oocytes) were also monitored for fluorescence. All fluorescence measurements were carried out at room temperature.

Fixation of oocytes for confocal imaging

Oocytes positive in fluorescence were incubated in 4% (v/v) paraformaldehyde, prepared in PBS, for 2 h at 4 °C and then washed in PBS. The oocytes were then manually sliced in half under a light microscope using a razor blade (thickness 0.1 mm) along the plane perpendicular to the boundary between the animal and vegetal hemispheres of the oocyte. This enabled both the animal and vegetal hemisphere, to be visualized together using confocal microscopy. The sliced oocytes were then mounted on a glass slide and visualized for GFP fluorescence by confocal microscopy as described previously using ×10, ×20 and ×40 objective lens. Confocal images were obtained using Adobe Photoshop software, version 3.0J.

Preparation of *X. laevis* oocyte microsomes

Approx. 20 *X. laevis* oocytes were homogenized in 4 vol. of ice-cold buffer A [50 mM Tris/HCl (pH 7.25)/250 mM sucrose/1 mM EGTA/1 mM dithiothreitol (DTT)/0.1 mM PMSF/10 μM leupeptin/1 μM pepstatin A]. The homogenate was centrifuged at 4500 ***g*** for 15 min and the resulting supernatant was aspirated and centrifuged at 160000 ***g*** for 1 h to pellet the microsomal fraction. All centrifugation procedures were carried out at 2 °C. The pellet was resuspended in buffer B [20 mM Tris/HCl (pH 7.25)/300 mM sucrose/1 mM EGTA/1 mM DTT/0.1 mM PMSF/10 μM leupeptin/1 μM pepstatin A], frozen in liquid nitrogen and stored at −80 °C until use. Protein estimations were carried out using a Bio-Rad Protein Assay reagent according to the manufacturers' instructions.

Na_2CO_3 extraction of microsomal membranes

Microsomal membranes were prepared as described previously and pellets were resuspended in 200 μl of 0.1 M Na_2CO_3 (pH 11) by repetitively passing through a needle (0.4 mm gauge), and incubated on ice for 30 min. Extracted proteins were separated from membrane bound proteins by centrifugation at 160000 ***g*** for 1 h at 2 °C. The resulting supernatant was carefully aspirated and the pellet resuspended in buffer B.

Gel and immunoblot analysis

Microsomal and soluble fractions were analysed by SDS/PAGE (7.5% gel) according to the method of Laemmli [20] (approx. 10 μg of protein per well). For immunoblotting, following electrophoresis proteins were transferred to a nitrocellulose membrane overnight at 2 °C as described in [21]. Nitrocellulose membranes were then blocked for 1 h at room temperature in 5% (w/v) skimmed milk in 0.1% (v/v) Tween 20/PBS. The nitrocellulose sheet was then washed in 0.1% Tween 20/PBS and the primary antibody, monoclonal antibody (mAb) 18A10 (raised against mouse type I Ins(1,4,5)P_3R [12]), was applied to the sheet for 1 h at room temperature. After washing the nitrocellulose membrane in 0.1% Tween 20/PBS, the membrane was incubated with secondary antibody (horseradish peroxidase conjugated with anti-rat IgG) for 1 h at room temperature. The membrane was then washed three times in 0.1% Tween 20/PBS, and the bound antibody (mAb18A10) was detected and visualized using the Enhanced Chemi-Luminescence system (ECL, Amersham, Bucks., U.K.).

Electron microscopic localization of chimeric protein by IgG–gold technique on frozen ultrathin sections

Frozen ultramicrotomy was performed as described by Tokuyasu [22], with some modifications. *Xenopus* eggs were fixed with fixative containing 4% paraformaldehyde and 0.02% (v/v) glutaraldehyde. After washing in PBS (pH 7.4), these eggs were embedded in PBS containing 10% (w/v) gelatin and 0.25% (w/v) agarose on ice. The eggs were cut into halves longitudinally, then incubated overnight in 2.3 M sucrose in 0.1 M sodium phosphate buffer (pH 7.4) containing 20% (v/v) polyvinylpyrrolidone, and rapidly frozen in liquid propane at −180 °C. Frozen ultrathin sections were cut with a Reichert Ultracut-E using a cryoattachment (FC-4D) at −80 °C to a thickness of approx. 95 nm. The sections were picked up on Formvar–carbon-coated nickel grids, incubated with 2% gelatin in PBS containing 10 mM glycine and 2% (w/v) normal goat serum, reacted for 60 min with either the antibody against Ins(1,4,5)P_3R (mAb18A10; 10 μg/ml), or non-immunized rat IgG. The sections were then washed six times with gelatin solution, and reacted for 15 min with gold particles conjugated with goat IgG against rat IgG (10 nm in diameter, $A_{525} = 0.08$; British BioCell, Cardiff, U.K.). After washing with sodium cacodylate buffer (pH 7.4), sections were post-fixed in 2% glutaraldehyde then in 1% (w/v) OsO_4, stained with uranyl acetate, embedded in LR White resin [23], and observed with a Hitachi H-7000 electron microscope.

Cross-linking experiment

Microsomal membranes from *X. laevis* oocytes were prepared as described previously and resuspended in 50 mM sodium phosphate (pH 8) to a concentration of 1 mg/ml. To 4 ml of resuspended microsomal membranes (typically containing 4 mg of protein), 1 ml of a stock solution of the cross-linking reagent DST (disuccinimidyl tartrate) (Pierce) was added to achieve a final concentration of 0.6, 1.7, 5 and 10 mM. The samples were then incubated on ice for 2 h and then subject to SDS/PAGE (5% gel) and immunoblotting using mAb18A10, as described previously.

RESULTS

Membrane association and homotetramer formation of GFP–Ins(1,4,5)P_3R(ES)

Using PCR, we created a chimeric fusion protein between GFP and a truncated Ins(1,4,5)P_3R mutant containing just the putative transmembrane spanning domain [amino acids 2216–2749; Ins(1,4,5)P_3R(ES)], which we microinjected into *X. laevis* oocytes. GFP was fused to the N-terminus of Ins(1,4,5)P_3R(ES) as depicted in Figure 1. In order to distinguish whether expressed GFP–Ins(1,4,5)P_3R(ES) was in fact expressed in cell membranes or in the cytoplasm, a *X. laevis* oocyte microsomal fraction (M) and a soluble cytosolic fraction (S) was prepared as described previously and subjected to immunoblotting with mAb18A10, which should recognize a portion of the C-terminal cytosolic

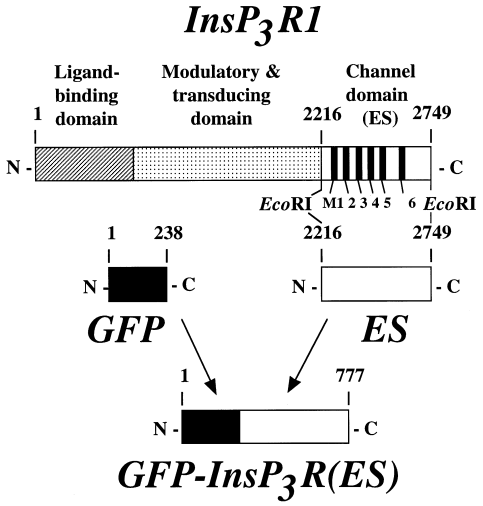

Figure 1 Construction of chimeric GFP–Ins(1,4,5)P_3R(ES) fusion protein

Using PCR, GFP was fused to the N-terminal end of a truncated type I Ins(1,4,5)P_3R mutant protein [Ins(1,4,5)P_3R(ES)], which contained just the putative transmembrane spanning domain (amino acids 2216–2749), with the large cytoplasmic N-terminal ligand binding and modulatory/transducing domains missing. (N-, N-terminus; C-, C-terminus; M1–6, putative transmembrane spanning domains 1–6.)

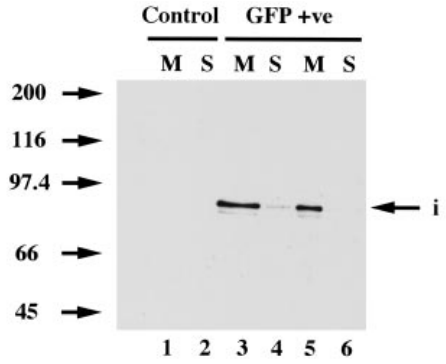

Figure 2 Western blot analysis of proteins expressed in *X. laevis* oocytes microinjected with pMT3GFP–Ins(1,4,5)P_3R(ES)

Microsomal membranes (M) and the soluble fraction (S) were separated as described in the Materials and methods section and subject to immunoblotting with mAb18A10. Lanes 1 and 2 represent *Xenopus* oocytes microinjected with just vector pMT3 (vector control) and lanes 3 and 4 represent oocytes microinjected with pMT3GFP–Ins(1,4,5)P_3R(ES), positive in GFP fluorescence. Lanes 5 and 6 represent microsomal and soluble fractions prepared from oocytes microinjected with pMT3GFP–Ins(1,4,5)P_3R(ES), after resuspension of microsomal membranes with 0.1 M Na_2CO_3. Lanes were loaded with 10 μg of protein and blots were developed using the ECL Western blotting system. The positions of the molecular mass markers are shown on the left (kDa) and a band immunoreactive to mAb 18A10 is denoted by 'i' on the right.

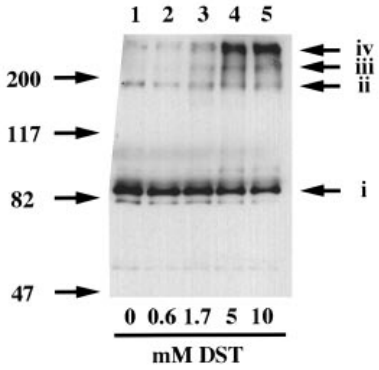

Figure 3 Cross-linking experiment on expressed GFP–Ins(1,4,5)P_3R(ES)

Microsomal membranes prepared from oocytes expressing GFP–Ins(1,4,5)P_3R(ES) were treated with the cross-linking reagent DST and were then subjected to SDS/PAGE and Western blot analysis using mAb18A10. Lanes 1–5 represent microsomal membranes incubated with 0, 0.6, 1.7, 5 and 10 mM DST respectively. The positions of molecular mass markers are shown on the left (kDa) and four bands immunoreactive with mAb18A10 (i, ii, iii and iv) shown on the right. Each lane contains 10 μg of protein and the blot was visualized using the ECL Western blotting system.

domain of the GFP–Ins(1,4,5)P_3R(ES) construct. Figure 2 shows the presence of an intense band of calculated molecular mass of approx. 80 kDa present in the microsomal fraction (M; lane 3) of oocytes microinjected with GFP–Ins(1,4,5)P_3R(ES) positive in GFP fluorescence, indicating the expression of GFP–Ins(1,4,5)P_3R(ES) (calculated molecular mass 77 kDa) in the microsomal membrane. Since Ins(1,4,5)P_3R(ES) contains two glycosylation sites, the predicted molecular mass is often slightly lower than the actual molecular mass. Note that in the soluble fraction (S) a very faint band is apparent of similar molecular mass to that observed in the microsomal fraction. Control oocytes microinjected with vector alone showed no such band in either microsomal (lane 1) or soluble (lane 2) fractions. The presence of immunoreactivity to mAb18A10 in the microsomal fraction of oocytes positive in GFP fluorescence indicates that the expressed protein is in fact associated with membranes. The presence of a very faint band in the soluble fraction (S; lane 4) probably represents contamination of the soluble fraction with protein from the microsomal fraction during the separation of these fractions. However, the presence of GFP–Ins(1,4,5)P_3R(ES) in the microsomal fraction cannot distinguish whether this protein is in fact integrated into the microsomal membrane or merely associated with this membrane.

In order to assess whether GFP–Ins(1,4,5)P_3R(ES) is in fact integrated into microsomal membranes, the microsomal fraction was resuspended in 0.1 M Na_2CO_3, which, due to the very alkaline conditions, will dissociate membrane-associated proteins while not affecting membrane-integrated proteins, leaving them anchored in the membrane [24]. Figure 2 (lanes 5 and 6) clearly shows the expressed protein to be located in the microsomal fraction after resuspension in Na_2CO_3, whilst no band immunoreactive with mAb18A10 is found in the soluble fraction (lane 6). This result demonstrates that the expressed protein is in fact membrane anchored and not merely membrane associated, and shows that targeting to internal membranes is not a result of a non-specific interaction between GFP and internal membranes.

In order to determine whether GFP–Ins(1,4,5)P_3R(ES) can form a homotetrameric complex like the wild-type (wt) type I Ins(1,4,5)P_3R, microsomal membranes prepared from oocytes microinjected with GFP–Ins(1,4,5)P_3R(ES) (positive in GFP fluorescence) were prepared and treated with increasing concentrations of the cross-linking reagent DST, and then subjected to SDS/PAGE gel electrophoresis and immunoblotting with mAb18A10. Figure 3 shows the presence of four bands of calculated molecular mass of approx. 85 kDa (i), 170 kDa (ii), 240 kDa (iii) and 325 kDa (iv), corresponding to predicted molecular masses for monomeric, homodimeric, homotrimeric and homotetrameric complexes respectively. The intensity of these bands increases with increasing DST concentration and clearly shows the presence of a protein with an expected molecular mass of a homotetrameric structure (iv), providing strong evidence that GFP–Ins(1,4,5)P_3R(ES) is able to form a homotetrameric structure like the wt type I Ins(1,4,5)P_3R, despite lacking the large N-terminal cytoplasmic domain.

Localization of expressed GFP–Ins(1,4,5)P_3R(ES) in *X. laevis* oocytes monitored using confocal microscopy

In order to monitor the intracellular localization of the mouse type I Ins(1,4,5)P_3R(ES), the chimeric GFP–Ins(1,4,5)P_3R(ES) fusion protein was expressed in *X. laevis* oocytes using the expression vector pMT3, allowing the intracellular distribution of expressed Ins(1,4,5)P_3Rs to be identified as areas of GFP fluorescence within the cell. Following microinjection, the eggs were incubated for 3 days in MBS and observed under a Zeiss confocal microscope using the $\times 10$ objective lens. Figure 4(A) shows an intact *X. laevis* oocyte microinjected with GFP–Ins(1,4,5)P_3R(ES) exhibiting GFP fluorescence under the pigmented animal pole (AP) of the oocyte. Little or no fluorescence signal was detected in the vegetal pole/hemisphere (VP) of the oocyte. Oocytes microinjected with pMT3 vector alone (vector control) typically showed very little fluorescence, comparable to background levels (results not shown).

In order to investigate the distribution of fluorescence in more detail, oocytes positive in fluorescence were fixed in 4% paraformaldehyde, sliced in half and observed using confocal microscopy. Figure 4(B) shows such an oocyte observed with the

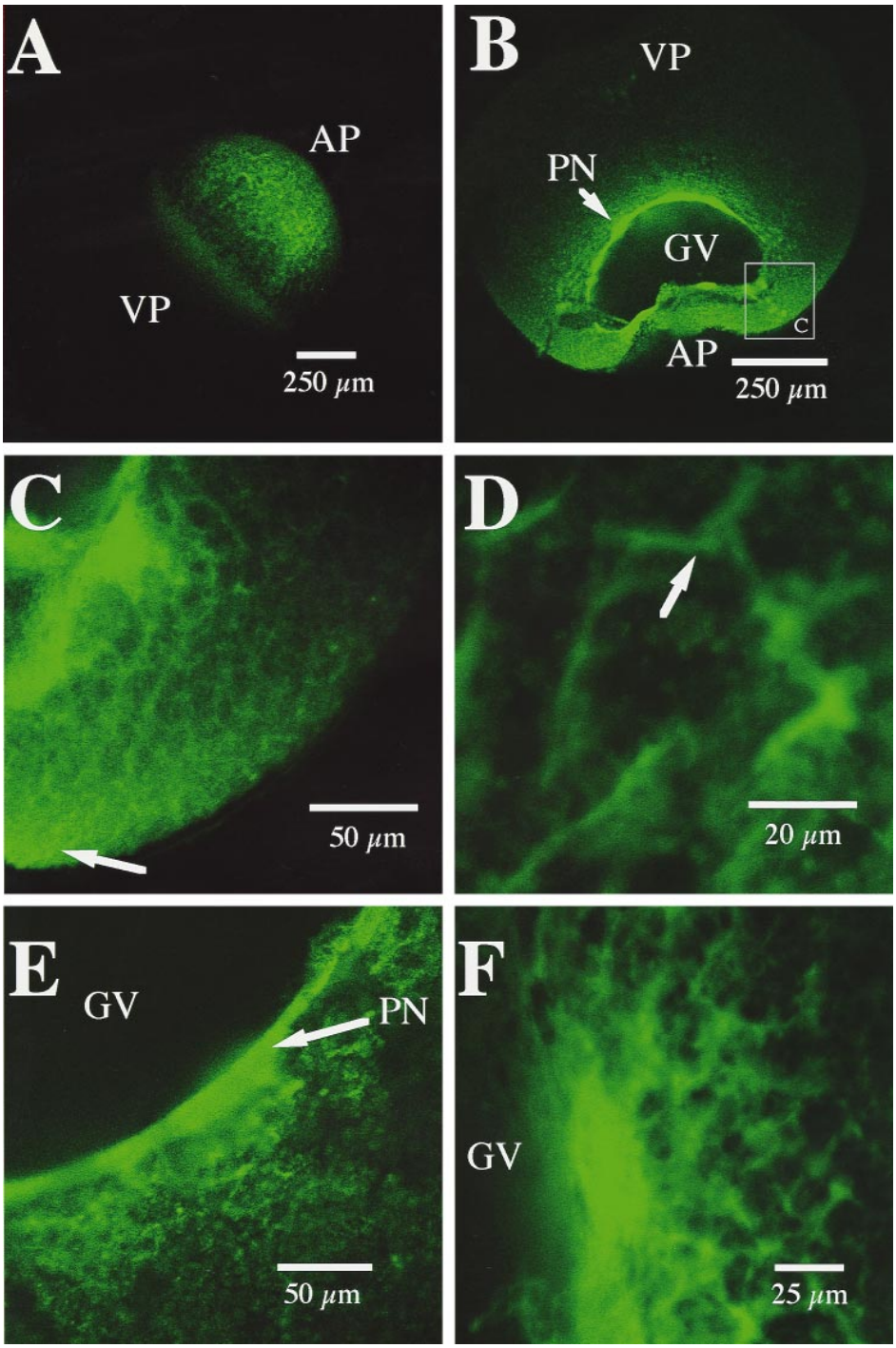

Figure 4 Localization of GFP–Ins(1,4,5)P_3R(ES) in *X. laevis* oocytes by fluorescence confocal microscopy

(**A**) Fluorescence observation of an intact, fully grown, stage VI *X. laevis* oocyte viewed under the ×10 objective lens 3 days after microinjection with GFP–Ins(1,4,5)P_3R(ES), demonstrating enriched fluorescence under the animal pole (AP) of the oocyte with very little detectable fluorescence under the vegetal pole (VP). (**B**) Intracellular observation of fluorescence viewed by the ×10 objective lens from an oocyte expressing GFP–Ins(1,4,5)P_3R(ES), sliced in half after fixation in 4% paraformaldehyde. Intense areas of fluorescence can be observed in the perinuclear region (PN, white arrow) and in regions of the animal pole under the plasma membrane of the oocyte. GV represents the germinal vesicle containing the oocyte nucleus. Little fluorescence can be observed in the vegetal hemisphere of the oocyte (VP). (**C**) Enlargement of a region (Figure 4**B**, box C) under the animal pole of the oocyte viewed by the ×20 objective lens, demonstrating a reticular network of fluorescence in the region between the germinal vesicle (top left) and plasma membrane. Note the intense fluorescence observed in the region lying just beneath the plasma membrane (depicted by the white arrow). (**D**) Enlargement of the reticular fluorescence pattern observed under the animal pole of the oocyte viewed under the ×40 objective lens. The white arrow depicts regions of intense fluorescence possibly representing intracellular membranes that form the site of GFP–Ins(1,4,5)P_3R(ES) targeting. (**E**) Enlargement of a portion of the germinal vesicle (GV) demonstrating intense fluorescence in the perinuclear region (PN) surrounding the oocyte nucleus (viewed under ×20 objective lens). Note the fluorescence labelling of structures closely associated with the perinuclear region that extends away from the germinal vesicle. (**F**) Enlargement of portion of the perinuclear region depicted by the white arrow in (**E**) (viewed under the ×40 objective lens). Note the intense fluorescence observed in the perinuclear region (PN) surrounding the germinal vesicle (GV), which appears to exhibit continuity with a reticular network of fluorescence distant from the germinal vesicle.

$\times 10$ objective lens, exhibiting an intense fluorescence signal under the animal pole (AP) of the cell, with greater intensity just under the plasma membrane and in the perinuclear region (PN). The fluorescence distribution pattern in the animal pole of the oocyte appears as a reticular-like network of fluorescence. To investigate the nature of the fluorescence distribution pattern observed in Figure 4(B), an area of the animal pole of the oocyte (C) was observed under the $\times 20$ objective lens (Figure 4C). Figure 4(C) shows a characteristic reticular-network of intense fluorescence, which is enriched in the perinuclear region (top left) and just beneath the plasma membrane (white arrow). This reticular fluorescence pattern extends from the perinuclear region to the plasma membrane and is highly suggestive of an ER-like distribution pattern of Ins(1,4,5)P_3R(ES). A previous immunocytochemical study has identified the endogenous *Xenopus* Ins(1,4,5)P_3R [*X*Ins(1,4,5)P_3R] on a characteristic ER-like reticular network under the animal pole of the oocyte, with increased intensity just beneath the plasma membrane and in the perinuclear region [25]. These results are consistent with our observations of an ER-like distribution pattern of GFP–Ins(1,4,5)P_3R(ES) under the animal pole of the oocyte.

The nature of this ER-like reticular pattern of fluorescence was further investigated by observation under the $\times 40$ objective lens (Figure 4D). Figure 4(D) shows the reticular fluorescence pattern at higher magnification ($\times 40$) and shows fluorescence localized on a reticular network of intracellular structures (depicted by the solid arrow), which exhibit a close proximity to each other and apparent continuity with similar adjacent structures. The dark areas between this reticular network may possibly represent yolk granules devoid of Ins(1,4,5)P_3Rs, which have previously been identified in *Xenopus* oocytes [25].

To investigate the nature of the fluorescence distribution pattern observed in the perinuclear region of the oocyte, a portion of this region was observed under the $\times 20$ objective lens. Figure 4(E) shows an intense fluorescence signal surrounding the germinal vesicle (depicted by the solid arrow), which houses the oocyte nucleus, possibly representing Ins(1,4,5)P_3Rs that are localized on the nuclear membrane or on membrane structures closely associated with this membrane, such as perinuclear ER.

Figure 4(F) shows a portion of the perinuclear region (depicted by the white arrow in Figure 4E) observed under the $\times 40$ objective lens and shows an intense pattern of fluorescence separating the germinal vesicle from the ER-like reticular network of fluorescence. The intense fluorescence signal in the perinuclear region extends away from the germinal vesicle and appears to exhibit continuity with an ER-like reticular network of fluorescence, possibly representing the localization of GFP–Ins(1,4,5)P_3R(ES) on nuclear membranes or on ER located in the perinuclear region. The apparent continuity of the perinuclear fluorescence with the reticular-like fluorescence further away from the perinuclear region suggests that perinuclear fluorescence may result from expressed Ins(1,4,5)P_3Rs located on perinuclear ER that exhibit membrane continuity with cytoplasmic ER, a possibility that is strengthened by a previous study locating the endogenous *Xenopus* Ins(1,4,5)P_3R on perinuclear ER [26].

It has previously been shown in our laboratory that expression of GFP alone in *Xenopus* oocytes leads to an even and non-localized distribution of GFP fluorescence within the oocyte [27], demonstrating that GFP alone does not mediate any specific intracellular targeting events. The striking localization of fluorescence from GFP–ES in the animal hemisphere of the oocyte on a reticular network of intracellular structures demonstrates that the ES fragment is in fact responsible for the targeting and localization of this fluorescence.

Subcellular localization of expressed GFP–Ins(1,4,5)P_3R(ES) in *X. laevis* oocytes using immunogold

Subcellular localization of expressed GFP–Ins(1,4,5)P_3R(ES) in *X. laevis* oocytes was further analysed by immunogold electron microscopy (Figure 5). Immunogold reacting with mAb18A10 were detected in frozen sections of oocytes expressing GFP–Ins(1,4,5)P_3R(ES) (Figure 5A), but not in those microinjected with the control vector (Figure 5B). Sections first reacted with non-immunized normal IgG did not display any significant immunogold staining (results not shown). The reacted immunogolds in sections of the expressed oocytes were mostly associated with membrane structures, probably the ER (Figure 5C), but were not localized in the mitochondria (Figure 5D) and plasma membranes (results not shown). These data indicate that the expressed chimeric GFP–Ins(1,4,5)P_3R(ES) proteins are functionally targeted to the ER like the intact Ins(1,4,5)P_3R.

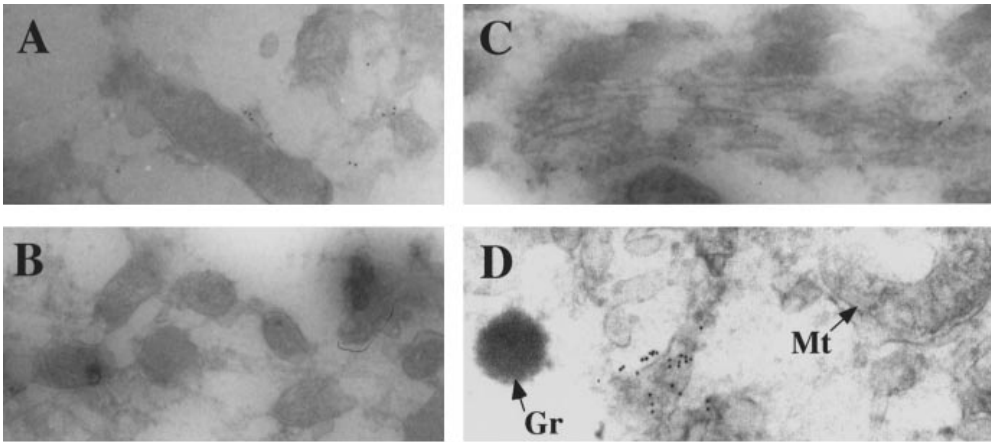

Figure 5 Subcellular localization of GFP–Ins(1,4,5)P_3R(ES) in *X. laevis* oocytes by immunogold electron microscopy

Frozen ultrathin sections ($\approx$ 95 nm thickness) of *X. laevis* oocytes were first reacted with mAb18A10, and then with gold particles (10 nm diameter) conjugated with anti-rat IgG. (**A**, **C**, **D**) Sections of oocytes expressed GFP–Ins(1,4,5)P_3R(ES). (**B**) Sections microinjected with the control vector. Gr, yolk granule; Mt, mitochondrion.

DISCUSSION

Here, we have employed the use of the GFP mutant S65T (replacement of Ser-65 with Thr) [28] to monitor the intracellular localization of a truncated mutant of the mouse type I Ins(1,4,5)P_3R [Ins(1,4,5)P_3R(ES)], containing only the putative transmembrane spanning region, which we expressed in *X. laevis* oocytes. Since the endogenous *X*Ins(1,4,5)P_3R has previously been shown to exhibit a selective localization to the ER under the animal pole of the oocyte and in the perinuclear region [25,26], the localization of expressed GFP–Ins(1,4,5)P_3R(ES) was considered to be an interesting question, particularly since the cytoplasmic N-terminal domain was missing.

Using confocal microscopy, we have demonstrated the localization of GFP fluorescence on reticular structures under the animal pole of the oocyte, with increased intensity in the perinuclear region and just beneath the plasma membrane. The reticular-like fluorescence pattern observed is suggestive of GFP–Ins(1,4,5)P_3R(ES) targeting to intracellular membranes, namely the ER, a possibility that is further strengthened by the demonstration that this chimeric construct is in fact membrane anchored. Enlargement of this reticular network (Figure 4D) shows fluorescence to be localized on defined intracellular structures, which appear to exhibit continuity with each other, and electron microscopic observations confirm that expressed GFP–Ins(1,4,5)P_3R(ES) is in fact localized on ER membranes, with mitochondrial and lysosomal membranes devoid of staining. The fact that expressed GFP–Ins(1,4,5)P_3R(ES) is selectively localized on ER under the animal pole of the oocyte like the endogenous *X*Ins(1,4,5)P_3R, provides circumstantial evidence that GFP–Ins(1,4,5)P_3R(ES) and *X*Ins(1,4,5)P_3R share similar targeting mechanisms and are in fact localized on the same Ca^{2+} store. The intense perinuclear fluorescence observed by confocal microscopy in our study may possibly represent GFP-Ins(1,4,5)P_3R(ES) localized on nuclear membranes or on membranes closely associated with nuclear membranes, such as perinuclear ER. A previous study locating the *X*Ins(1,4,5)P_3R to perinuclear ER [26], and the apparent continuity of perinuclear fluorescence with cytoplasmic reticular fluorescence, suggesting membrane continuity between targeted perinuclear and cytoplasmic membranes, favours localization on perinuclear ER membranes.

It has already been established that Ins(1,4,5)P_3R can exist as a homotetrameric and, more recently, heterotetrameric complex in the membranes of Ins(1,4,5)P_3-sensitive Ca^{2+} stores [14]. However, the mechanisms and regions of the Ins(1,4,5)P_3R involved in homotetramer formation remain poorly understood. Cross-linking experiments in our study demonstrate that GFP–Ins(1,4,5)P_3R(ES) is able to form a homotetrameric complex. Our finding provides direct evidence that homotetramer formation can be mediated by the transmembrane spanning region alone, which also contains the cytoplasmic C-terminal region of the Ins(1,4,5)P_3R, and can occur without the requirement for the large N-terminal cytoplasmic region. The possibility that expressed GFP–Ins(1,4,5)P_3R(ES) can form a heterotetrameric complex with endogenous *X*Ins(1,4,5)P_3R is currently being investigated. However, the cross-linking experiment did not reveal the presence of any bands of calculated molecular masses for heterotetramer formation with endogenous *X*Ins(1,4,5)P_3R. The possibility exists that ER targeting and tetrameric complex formation are coupled processes, such that tetramer formation promotes ER retention. Since the endogenous *X*Ins(1,4,5)P_3R is targeted to the ER, it is possible that heterotetramer formation between GFP–Ins(1,4,5)P_3R(ES) and *X*Ins(1,4,5)P_3R is responsible for targeting of GFP–Ins(1,4,5)P_3R(ES) to the ER. However, the absence of any bands of calculated molecular masses of a heterotetramer in the cross-linking experiment discredits this theory and supports ER retention of Ins(1,4,5)P_3R(ES) without a requirement for the *X*Ins(1,4,5)P_3R. Since GFP–Ins(1,4,5)P_3R(ES) contains no ligand binding site and is presumably non-functional, it will be interesting to see what effect expression of GFP–Ins(1,4,5)P_3R(ES) in *Xenopus* oocytes has on intracellular Ca^{2+} dynamics, in particular Ins(1,4,5)P_3-induced Ca^{2+} release.

The mechanisms of protein targeting to ER membranes are not completely understood. However, several targeting sequences have been described for several ER-resident proteins, including the KDEL/HDEL sequence, which promotes the retention of luminal ER proteins [29], a dilysine motif at the COOH terminus, which has been strongly implicated in ER targeting [30], and the KKXX/KXKXX (or a close variation on this sequence) sequences, which are commonly found in ER-membrane-targeted proteins [29]. What is emerging is that multiple signals may mediate ER targeting and that a single protein may contain several such signals that act in concert to target the protein to the ER. The action of these signals is unknown, but the current belief is that these signals promote retrieval of ER-resident membrane proteins from post-ER organelles [30]. Analysis of the amino acid sequence of the type I Ins(1,4,5)P_3R reveals several signals that could potentially contribute to or mediate retention in the ER. The presence of a dilysine motif close to the COOH terminus at amino acid position 2734, a KQKQ (amino acid position 2727) and a KKEE (amino acid position 2601) sequence, both present in the COOH terminal region, plus several dilysine motifs located in the putative transmembrane spanning domains, may play a role in ER retention of the Ins(1,4,5)P_3R. These sequences are conserved among type I Ins(1,4,5)P_3Rs from mouse, rat, human and *Xenopus* and are all present in the GFP–Ins(1,4,5)P_3R(ES) construct.

Our results provide evidence that the Ins(1,4,5)P_3R(ES) segment alone, containing the putative transmembrane spanning region and C-terminal cytoplasmic domain, is capable of directing intracellular targeting to the ER and therefore may contain an ER targeting/retention signal. The ability of chimeric GFP–Ins(1,4,5)P_3R(ES) to form a homotetrameric complex suggests that the ES region of the Ins(1,4,5)P_3R is sufficient to mediate this process, also implicating a role for the transmembrane spanning domain and C-terminal region in homotetrameric complex formation. Moreover, this study has paved the way for subsequent studies on the effects of mutation of the ES segment in order to further define the structural requirements necessary for ER targeting.

We thank Dr. Shoen Kume for critical comments on the manuscript, Dr. Hideaki Mizuno for valuable assistance in the preparation of confocal images, Dr. Julie Matheson for valuable assistance in the procurement of *X. laevis* oocytes and Miss Kaori Kawamoto for her valuable secretarial assistance. This work was supported by grants from the Ministry of Education, Science, Sports and Culture of Japan, the Ministry of Health and Welfare of Japan, and RIKEN (the Institute of Physical and Chemical Research). L.G.S. is a Science and Technology Agency of Japan (S.T.A.) research fellow.

REFERENCES

1 Berridge, M. J. (1993) Nature (London) **361**, 315–325
2 Berridge, M. J. and Irvine, R. F. (1989) Nature (London) **341**, 197–205
3 Furuichi, T., Yoshikawa, S., Miyawaki, A., Wada, K., Maeda, N. and Mikoshiba, K. (1989) Nature (London) **342**, 32–38
4 Furuichi, T., Kohda, K., Miyawaki, A. and Mikoshiba, K. (1994) Curr. Opin. Neurobiol. **4**, 294–303
5 Blondel, O., Takeda, J., Janssen, H., Seino, S. and Bell, G. I. (1993) J. Biol. Chem. **268**, 11356–11363

6 Worley, P. F., Baraban, J. M., Supattapone, S., Wilson, V. S. and Snyder, S. H. (1987) J. Biol. Chem. **262**, 12132–12136
7 Mignery, G. A., Südhof, T. C., Takei, K. and De Camilli, P. (1989) Nature (London) **342**, 192–195
8 Otsu, H., Yamamoto, A., Maeda, N., Mikoshiba, K. and Tashiro, Y. (1990) Cell Struct. Funct. **15**, 163–173
9 Satoh, T., Ross, C. A., Villa, A., Supattapone, S., Pozzan, T., Snyder, S. H. and Meldolesi, J. (1990) J. Cell Biol. **111**, 615–624
10 Ross, C. A., Danoff, S. K., Schell, M. J., Snyder, S. H. and Ullrich, A. (1992) Proc. Natl. Acad. Sci. U.S.A. **89**, 4265–4269
11 Maeda, N., Kawasaki, T., Nakade, S., Yokota, N., Taguchi, T., Kasai, M. and Mikoshiba, K. (1991) J. Biol. Chem. **266**, 1109–1116
12 Maeda, N., Niinobe, M. and Mikoshiba, K. (1990) EMBO J. **9**, 61–67
13 Mignery, G. A. and Südhof, T. C. (1990) EMBO J. **9**, 3893–3898
14 Monkawa, T., Miyawaki, A., Sugiyama, T., Yoneshima, H., Yamamoto-Hino, M., Furuichi, T., Saruta, T., Hasegawa, M. and Mikoshiba, K. (1995) J. Biol. Chem. **270**, 14700–14704
15 Miyawaki, A., Furuichi, T., Ryou, Y., Yoshikawa, S., Nakagawa, T., Saitoh, T. and Mikoshiba, K. (1991) Proc. Natl. Acad. Sci. U.S.A. **88**, 4911–4915
16 Meldolesi, J., Madeddu, L. and Pozzan, T. (1990) Biochim. Biophys. Acta **1055**, 130–140
17 Pozzan, T., Rizzuto, R., Volpe, P. and Meldolesi, J. (1994) Physiol. Rev. **74**, 595–636
18 Prasher, D. C., Eckenrode, V. K., Ward, W. W., Prendergast, F. G. and Cormier, M. J. (1992) Gene **111**, 229–233
19 Colman, A. (1984) Transcription and Translation: a Practical Approach, pp. 271–302, IRL Press, Oxford
20 Laemmli, U. K. (1970) Nature (London) **227**, 680–685
21 Towbin, H. T., Staehelin, T. and Gordon, J. (1979) Proc. Natl. Acad. Sci. U.S.A. **76**, 4350–4554
22 Tokuyasu, K. T. (1989) Histochem. J. **21**, 163–171
23 Tokuyasu, K. T. (1986) J. Microsc. **143**, 139–141
24 Foletti, D., Guerini, D. and Carafoli, E. (1995) FASEB J. **9**, 670–680
25 Kume, S., Muto, A., Aruga, J., Nakagawa, T., Michikawa, T., Furuichi, T., Nakade, S., Okano, H. and Mikoshiba, K. (1993) Cell **73**, 555–570
26 Parys, J. B., Sernett, S. W., DeLisle, S., Snyder, P. M., Welsh, M. J. and Campbell, K. P. (1992) J. Biol. Chem. **267**, 18776–18782
27 Matheson, J. M., Miyawaki, A., Muto, A., Inoue, T. and Mikoshiba, K. (1996) Biomed. Res. **17**, 221–225
28 Cubitt, A. B., Heim, R., Adams, S. R., Boyd, A. E., Gross, L. A. and Tsien, R. Y. (1995) Trends Biochem. Sci. **20**, 448–455
29 Pelham, H. R. B. and Munro, S. (1993) Cell **75**, 603–605
30 Lorenzen, J. A., Dadabay, C. Y. and Fischer, E. (1995) J. Cell Biol. **131**, 631–643

Received 24 October 1996/19 November 1996; accepted 3 December 1996